50. Neutrino Cross Section Measurements

Revised August 2015 by G.P. Zeller (Fermilab)

Neutrino cross sections are an essential ingredient in all neutrino experiments. Interest in neutrino scattering has recently increased due to the need for such information in the interpretation of neutrino oscillation data. Historically, neutrino scattering results on both charged current (CC) and neutral current (NC) channels have been collected over many decades using a variety of targets, analysis techniques, and detector technologies. With the advent of intense neutrino sources constructed for neutrino oscillation investigations, experiments are now remeasuring these cross sections with a renewed appreciation for nuclear effects† and the importance of improved neutrino flux estimations. This work summarizes accelerator-based neutrino cross section measurements performed in the $\sim 0.1 - 300$ GeV range with an emphasis on inclusive, quasi-elastic, and pion production processes, areas where we have the most experimental input at present (Table 50.1 and Table 50.2). For a more comprehensive discussion of neutrino cross sections, including neutrino-electron elastic scattering and lower energy neutrino measurements, the reader is directed to a recent review of this subject [1]. Here, we survey existing experimental data on neutrino interactions and do not attempt to provide a census of the associated theoretical calculations, which are both important and plentiful.

Table 50.1: List of beam properties, nuclear targets, and durations for modern accelerator-based neutrino experiments studying neutrino scattering.

Experiment	beam	$\langle E_\nu \rangle$, $\langle E_{\overline{\nu}} \rangle$ GeV	neutrino target(s)	run period
ArgoNeuT	$\nu, \overline{\nu}$	4.3, 3.6	Ar	2009 – 2010
ICARUS	ν	20.0	Ar	2010 – 2012
K2K	ν	1.3	CH, H_2O	2003 – 2004
MicroBooNE	ν	0.8	Ar	2015 –
MINERvA	$\nu, \overline{\nu}$	3.5 (LE), 5.5 (ME)	He, CH, H_2O, Fe, Pb	2009 –
MiniBooNE	$\nu, \overline{\nu}$	0.8, 0.7	CH_2	2002 – 2012
MINOS	$\nu, \overline{\nu}$	3.5, 6.1	Fe	2004 –
NOMAD	$\nu, \overline{\nu}$	23.4, 19.7	C	1995 – 1998
NOvA	$\nu, \overline{\nu}$	2.0, 2.0	CH_2	2010 –
SciBooNE	$\nu, \overline{\nu}$	0.8, 0.7	CH	2007 – 2008
T2K	$\nu, \overline{\nu}$	0.6, 0.6	CH, H_2O	2010 –

† Nuclear effects refer to kinematic and final state effects which impact neutrino scattering off nuclei. Such effects can be significant and are particularly relevant given that modern neutrino experiments make use of nuclear targets to increase their event yields.

Table 50.2: Summary of published neutrino cross section measurements from modern accelerator-based experiments. All measurements are ν_μ or $\overline{\nu}_\mu$ scattering with the exception of the last column which is a ν_e measurement.

Experiment	inclusive	0π	$\pi^\pm$	π^0	ν_e
ArgoNeuT	CC [2,3]	2p [4]	CC [5]	–	–
K2K	–	CC [6]	CC[7,8]	CC [9], NC [10]	–
MINERνA	CC [11]	CC[12,13], 1p[14]	CC [15]	CC [16]	–
MiniBooNE	–	CC [17,18], M_A [19], NC[20,21,22]	CC [23,24]	CC [25], NC [26,27]	–
MINOS	CC [28]	M_A[29]	–	–	–
NOMAD	CC [30]	CC [31]	–	NC [32]	–
SciBooNE	CC [33]	–	CC [34]	NC [35,36]	–
T2K	CC [37,38]	CC [39], NC [40]	–	–	CC[41]

50.1. Inclusive Scattering

Over the years, many experiments have measured the total inclusive cross section for neutrino ($\nu_\mu N \to \mu^- X$) and antineutrino ($\overline{\nu}_\mu N \to \mu^+ X$) scattering off nucleons covering a broad range of neutrino energies. As can be seen in Fig. 50.1, the inclusive cross section approaches a linear dependence on neutrino energy. Such behavior is expected for point-like scattering of neutrinos from quarks, an assumption which breaks down at lower energies. To provide a more complete picture, differential cross sections for such inclusive scattering processes have been reported – these include measurements on iron from NuTeV [42] and, more recently, at lower neutrino energies on argon from ArgoNeuT [2,3] and on carbon from T2K [37]. MINERvA has also provided new measurements of the ratios of the muon neutrino CC inclusive scattering cross section on a variety of nuclear targets such as lead, iron, and carbon [11]. At high energy, the inclusive cross section is dominated by deep inelastic scattering (DIS). Several high energy neutrino experiments have measured the DIS cross sections for specific final states, for example opposite-sign dimuon production. The most recent dimuon cross section measurements include those from CHORUS [43], NOMAD [44], and NuTeV [45]. At lower neutrino energies, the inclusive cross section is an additionally complex combination of quasi-elastic scattering

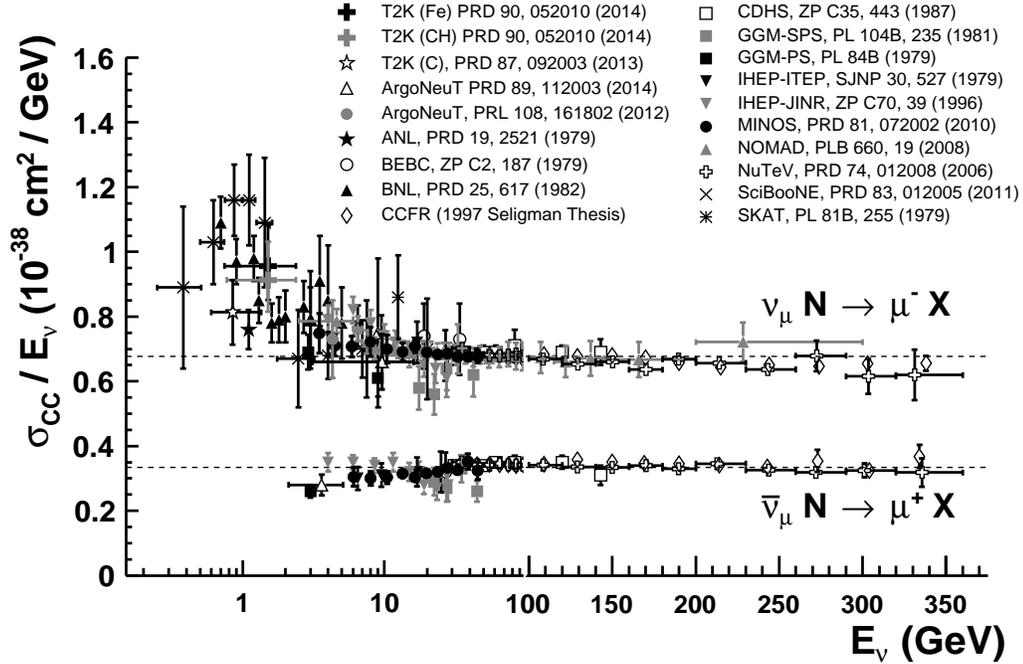and pion production processes, two areas we discuss next.

Figure 50.1: Measurements of ν_μ and $\overline{\nu}_\mu$ CC inclusive scattering cross sections (per nucleon) divided by neutrino energy as a function of neutrino energy. Note the transition between logarithmic and linear scales occurring at 100 GeV. Neutrino cross sections are typically twice as large as their corresponding antineutrino counterparts, although this difference can be larger at lower energies. NC cross sections (not shown) are generally smaller but non-negligible compared to the CC scattering case.

50.2. Quasi-elastic scattering

Quasi-elastic (QE) scattering is the dominant neutrino interaction for neutrino energies less than ~ 1 GeV and represents a large fraction of the signal samples in many neutrino oscillation experiments. Historically, neutrino (antineutrino) quasi-elastic scattering refers to the process, $\nu_\mu\, n \to \mu^-\, p$ $(\overline{\nu}_\mu\, p \to \mu^+\, n)$, where a charged lepton and single nucleon are ejected in the elastic interaction of a neutrino (or antineutrino) with a nucleon in the target material. This is the final state one would strictly observe, for example, in scattering off of a free nucleon target. Fig. 50.2 displays the current status of existing measurements of ν_μ and $\overline{\nu}_\mu$ QE scattering cross sections as a function of neutrino energy. In this plot, and all others in this review, the prediction from a representative neutrino event generator (NUANCE) [46] provides a theoretical comparator. Other generators and more sophisticated calculations exist which can yield significantly different predictions [47]. Note that modern experiments have recently opted to report QE cross sections as a function of final state muon or proton kinematics [17,18,48]. Such

distributions are more difficult to compare between experiments but are much less model-dependent and provide more stringent tests of the theory than cross sections as a function of neutrino energy (E_ν) or 4-momentum transfer (Q^2).
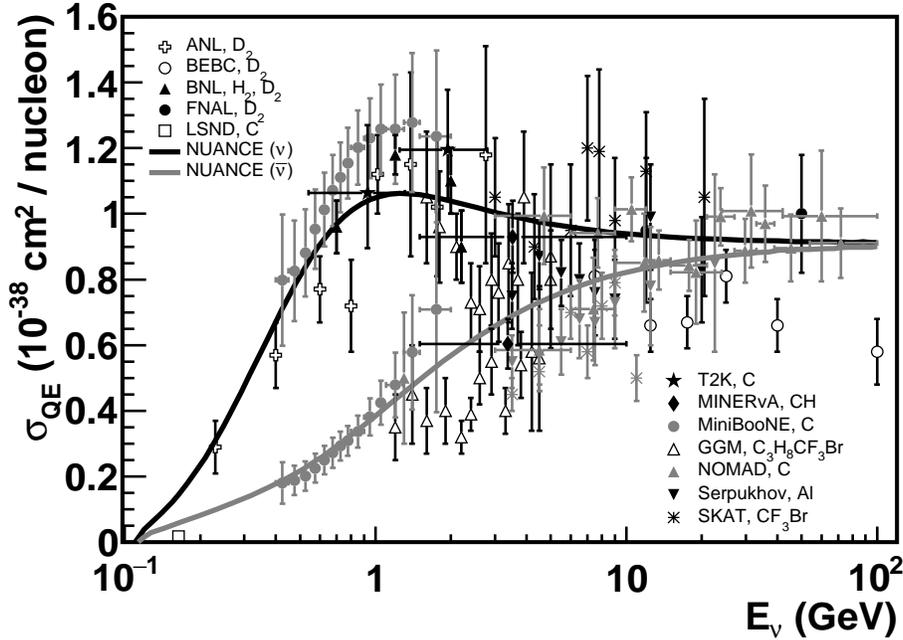

Figure 50.2: Measurements of ν_μ (black) and $\overline{\nu}_\mu$ (red) QE scattering cross sections (per nucleon) as a function of neutrino energy. Data on a variety of nuclear targets are shown, including measurements from ANL [49], BEBC [50], BNL [51], FNAL [52], LSND [53], T2K [39], MINERvA [12], MiniBooNE [17,18], GGM [54], NOMAD [31], Serpukhov [55], and SKAT [56]. Shown is the QE free nucleon scattering prediction from NUANCE [46] assuming $M_A = 1.0$ GeV. This prediction is significantly altered by nuclear effects in the case of neutrino-nucleus scattering. Although plotted together, care should be taken in interpreting measurements performed on targets heavier than D_2 due to possible differences in QE identification and kinematics.

In many of these initial measurements of the neutrino QE cross section, bubble chamber experiments employed light targets (H_2 or D_2) and required both the detection of the final state muon and single nucleon‡; thus the final state was clear and elastic kinematic conditions could be verified. The situation is more complicated, of course, for heavier nuclear targets. In this case, nuclear effects can impact the size and shape of the cross section as well as the final state kinematics and topology. Due to intranuclear hadron rescattering and the possible effects of correlations between target nucleons, additional nucleons may be ejected in the final state; hence, a QE interaction on a nuclear target does not always imply the ejection of a *single* nucleon. One therefore needs to take some care in defining what one means by neutrino QE scattering when scattering

---

‡ In the case of D_2, many experiments additionally observed the spectator proton.

off targets heavier than H_2 or D_2. Adding to the complexity, recent MiniBooNE measurements of the ν_μ and $\overline{\nu}_\mu$ QE scattering cross sections on carbon near 1 GeV have revealed a significantly larger cross section than originally anticipated [17,18]. Such an enhancement was observed many years prior in electron-nucleus scattering [57] and is believed to be due to the presence of correlations between target nucleons in the nucleus. As a result, the impact of such nuclear effects on neutrino QE scattering has recently been the subject of intense experimental and theoretical scrutiny with potential implications on event rates, nucleon emission, neutrino energy reconstruction, and neutrino/antineutrino ratios. The reader is referred to a recent review of the situation in [58,59]. Additional measurements are clearly needed before a complete understanding is achieved. To help drive further progress, neutrino-nucleus QE cross sections have been reported for the first time in the form of double-differential distributions in muon kinematics, $d^2\sigma/dT_\mu d\cos\theta_\mu$, by MiniBooNE [17,18] thus reducing the model-dependence of the reported data and allowing a more rigorous two-dimensional test of the underlying nuclear theory. Experiments such as ArgoNeuT have begun to provide the first measurements of proton multiplicities in neutrino-argon QE scattering [4,48], a critical ingredient in understanding the hadronic side of these interactions and final state effects. MINOS, NOvA, and T2K have started to study QE interactions in their near detectors with sizable statistics [29,39,60]. Most recently, MINERvA has measured the differential cross section, $d\sigma/dQ^2_{QE}$, ν_e QE scattering [61], single proton emission [14], and vertex energy in both ν_μ and $\overline{\nu}_\mu$ QE interactions in hydrocarbon [12,13]. With the MiniBooNE results having revealed additional complexities in the QE channel, measurements from other neutrino experiments are crucial for getting a better handle on the underlying nuclear physics impacting neutrino-nucleus interactions. What we once thought was "simple" QE scattering is in fact not so simple.

In addition to such charged current investigations, measurements of the neutral current counterpart of this channel have also been performed. The most recent NC elastic scattering cross section measurements include those from BNL E734 [62], MiniBooNE [20,21,22], and T2K [40]. A number of measurements of the Cabibbo-suppressed antineutrino QE hyperon production cross section have additionally been reported [56,63], although not in recent years.

50.3. Pion Production

In addition to such elastic processes, neutrinos can also inelastically scatter producing a nucleon excited state (Δ, N^*). Such baryonic resonances quickly decay, most often to a nucleon and single-pion final state. Historically, experiments have measured various exclusive final states associated with these reactions, the majority of which have been on hydrogen and deuterium targets [1].

In addition to such resonance production processes, neutrinos can also coherently scatter off of the entire nucleus and produce a distinctly forward-scattered single pion final state. Both CC ($\nu_\mu A \rightarrow \mu^- A \pi^+$, $\overline{\nu}_\mu A \rightarrow \mu^+ A \pi^-$) and NC ($\nu_\mu A \rightarrow \nu_\mu A \pi^0$, $\overline{\nu}_\mu A \rightarrow \overline{\nu}_\mu A \pi^0$) processes are possible in this case. Even though the level of coherent pion production is small compared to resonant processes, observations exist across a broad energy range and
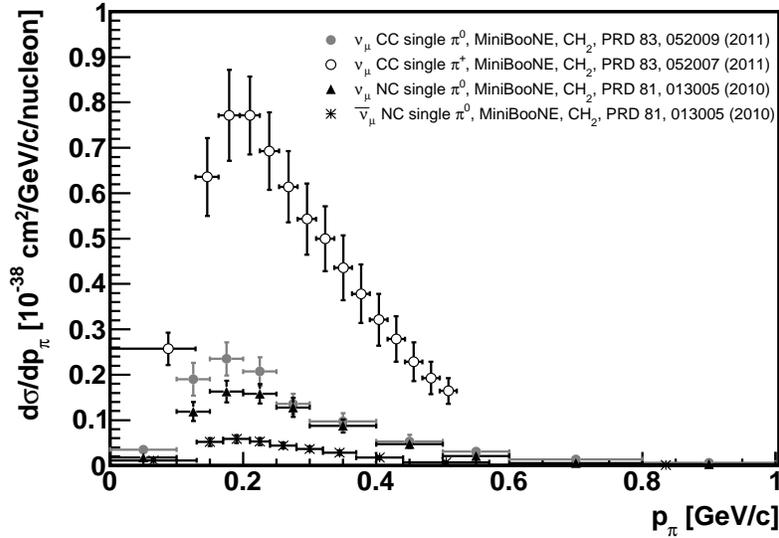
Figure 50.3: Differential cross sections for CC and NC pion production from MiniBooNE at a mean neutrino energy of 0.8 GeV. Shown here are the measurements as a function of the momentum of the outgoing pion in the interaction, a kinematic that is particularly sensitive to final state interactions. Other distributions are also available in the publications listed in the legend.

on multiple nuclear targets [64]. More recently, several modern neutrino experiments have measured coherent pion production cross sections including ArgoNeuT [5], K2K [8], MINERvA [15], MiniBooNE [27], MINOS [65], NOMAD [32], and SciBooNE [34,36].

As with QE scattering, a new appreciation for the significance of nuclear effects has surfaced in pion production channels, again due to the use of heavy nuclear targets in modern neutrino experiments. Many experiments have been careful to report cross sections for various detected final states, thereby not correcting for large and uncertain nuclear effects (e.g., pion rescattering, charge exchange, and absorption) which can introduce unwanted sources of uncertainty and model dependence. Recent measurements of single-pion cross sections, as published by K2K [9,10], MiniBooNE [24], and SciBooNE [35], take the form of ratios with respect to QE or CC inclusive scattering samples. Providing the most comprehensive survey of neutrino single-pion production to date, MiniBooNE has recently published a total of 16 single- and double-differential cross sections for both the final state muon (in the case of CC scattering) and pion in these interactions; thus, providing the first measurements of these distributions (Fig. 50.3) [23–26]. MINERvA has recently produced similar kinematic measurements at higher neutrino energies (Fig. 50.4) [16,66]. Regardless of the interaction channel, such differential cross section measurements (in terms of observed final state particle kinematics) are now preferred for their reduced model dependence and for the additional kinematic information they provide. Such a new direction has been the focus of modern measurements as opposed to the reporting of more model-dependent, historical cross sections as a function of E_ν or Q^2. Together with similar results for other interaction channels, a better understanding and modeling of nuclear effects will be possible moving forward.
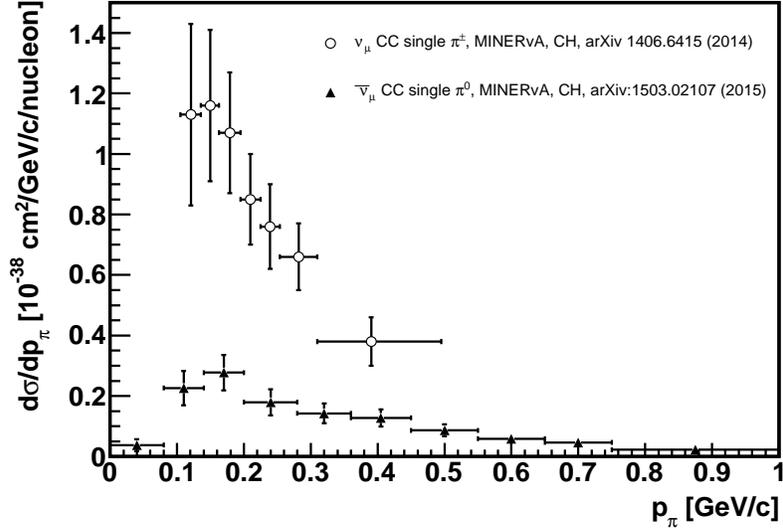
Figure 50.4: Differential cross sections for neutrino and antineutrino pion production from MINERvA at a mean neutrino energy of 3.3 GeV. Shown here are the measurements as a function of the momentum of the outgoing pion in the interaction, a kinematic that is particularly sensitive to final state interactions. Other distributions are also available in the publications listed in the legend. Note that while the MINERvA ν_μ measurement includes both π^+ and π^- production, the sample is almost entirely ($> 99\%$) π^+ final states.

It should be noted that baryonic resonances can also decay to multi-pion, other mesonic (K, η, ρ, etc.), and even photon final states. Experimental results for these channels are typically sparse or non-existent [1]; however, photon production processes can be an important background for $\nu_\mu \rightarrow \nu_e$ appearance searches and thus have become the focus of some recent experimental investigations; for example, in NOMAD [67].

50.4. Outlook

Currently operating experiments will continue to produce additional neutrino cross section measurements as they accumulate additional statistics, while a few new experiments will soon be coming online. In the coming years, analysis of a broad energy range of data on a variety of targets in the MINERvA experiment will provide the most detailed analysis yet of nuclear effects in neutrino interactions. Data from ArgoNeuT, ICARUS, MicroBooNE, and SBND will probe deeper into complex neutrino final states using the superior capabilities of liquid argon time projection chambers, while the T2K and NOvA near detectors will collect high statistics samples in intense neutrino beams. Together, these investigations should significantly advance our understanding of neutrino-nucleus scattering in the next decade.

50.5.   Acknowledgments

References:
 1.   J.A. Formaggio and G.P. Zeller, Rev. Mod. Phys. **84**, 1307 (2012).
 2.   C. Anderson *et al.*, Phys. Rev. Lett. **108**, 161802 (2012).
 3.   R. Acciarri *et al.*, Phys. Rev. **D89**, 112003 (2014).
 4.   R. Acciarri *et al.*, Phys. Rev. **D90**, 012008 (2014).
 5.   R. Acciarri *et al.*, Phys. Rev. Lett. **113**, 261801 (2014).
 6.   R. Gran *et al.*, Phys. Rev. **D74**, 052002 (2006).
 7.   A. Rodriguez *et al.*, Phys. Rev. **D78**, 032003 (2008).
 8.   M. Hasegawa *et al.*, Phys. Rev. Lett. **95**, 252301 (2005).
 9.   C. Mariani *et al.*, Phys. Rev. **D83**, 054023 (2011).
10.   S. Nakayama *et al.*, Phys. Lett. **B619**, 255 (2005).
11.   B.G. Tice *et al.*, Phys. Rev. Lett. **112**, 231801 (2014).
12.   G.A. Fiorentini *et al.*, Phys. Rev. Lett. **111**, 022502 (2013).
13.   L. Fields *et al.*, Phys. Rev. Lett. **111**, 022501 (2013).
14.   T. Walton *et al.*, Phys. Rev. **D91**, 071301 (2015).
15.   A. Higuera *et al.*, Phys. Rev. Lett. **113**, 261802 (2014).
16.   T. Le *et al.*, Phys. Lett. **B749**, 130 (2015).
17.   A.A. Aguilar-Arevalo *et al.*, Phys. Rev. **D81**, 092005 (2010).
18.   A.A. Aguilar-Arevalo *et al.*, Phys. Rev. **D88**, 032001 (2013).
19.   A.A. Aguilar-Arevalo *et al.*, Phys. Rev. Lett. **100**, 032301 (2008).
20.   A.A. Aguilar-Arevalo *et al.*, Phys. Rev. **D82**, 092005 (2010).
21.   A.A. Aguilar-Arevalo *et al.*, Phys. Rev. **D91**, 012004 (2015).
22.   A.A. Aguilar-Arevalo *et al.*, Phys. Rev. **D91**, 012004 (2015).
23.   A.A. Aguilar-Arevalo *et al.*, Phys. Rev. **D83**, 052007 (2011).
24.   A.A. Aguilar-Arevalo *et al.*, Phys. Rev. Lett. **103**, 081801 (2009).
25.   A.A. Aguilar-Arevalo *et al.*, Phys. Rev. **D83**, 052009 (2011).
26.   A.A. Aguilar-Arevalo *et al.*, Phys. Rev. **D81**, 013005 (2010).
27.   A.A. Aguilar-Arevalo *et al.*, Phys. Lett. **B664**, 41 (2008).
28.   P. Adamson *et al.*, Phys. Rev. **D81**, 072002 (2010).
29.   P. Adamson *et al.*, Phys. Rev. **91**, 012005 (2015).
30.   Q. Wu *et al.*, Phys. Lett. **B660**, 19 (2008).
31.   V. Lyubushkin *et al.*, Eur. Phys. J. **C63**, 355 (2009).
32.   C.T. Kullenberg *et al.*, Phys. Lett. **B682**, 177 (2009).
33.   Y. Nakajima *et al.*, Phys. Rev. **D83**, 12005 (2011).
34.   K. Hiraide *et al.*, Phys. Rev. **D78**, 112004 (2008).
35.   Y. Kurimoto *et al.*, Phys. Rev. **D81**, 033004 (2010).
36.   Y. Kurimoto *et al.*, Phys. Rev. **D81**, 111102 (R)(2010).
37.   K. Abe *et al.*, Phys. Rev. **D87**, 092003 (2013).
38.   K. Abe *et al.*, Phys. Rev. **D90**, 052010 (2014).

39. K. Abe *et al.*, Phys. Rev. **D91**, 112002 (2015).
40. K. Abe *et al.*, Phys. Rev. **D90**, 072012 (2014).
41. K. Abe *et al.*, Phys. Rev. Lett. **113**, 241803 (2014).
42. M. Tzanov *et al.*, Phys. Rev. **D74**, 012008 (2006).
43. A. Kayis-Topaksu *et al.*, Nucl. Phys. **B798**, 1 (2008).
44. O. Samoylov *et al.*, Nucl. Phys. **B876**, 339 (2013).
45. D. Mason *et al.*, Phys. Rev. Lett. **99**, 192001 (2007).
46. D. Casper, Nucl. Phys. (Proc. Supp.) **112**, 161 (2002), default v3 NUANCE.
47. R. Tacik, AIP Conf. Proc. **1405**,229(2011); S. Boyd *et al.*, AIP Conf. Proc. **1189**, 60(2009).
48. O. Palamara *et al.*, arXiv:1309.7480 [physics.ins-det].
49. S.J. Barish *et al.*, Phys. Rev. **D16**, 3103 (1977).
50. D. Allasia *et al.*, Nucl. Phys. **B343**, 285 (1990).
51. N.J. Baker *et al.*, Phys. Rev. **D23**, 2499 (1981); G. Fanourakis *et al.*, Phys. Rev. **D21**, 562 (1980).
52. T. Kitagaki *et al.*, Phys. Rev. **D28**, 436 (1983).
53. L.B. Auerbach *et al.*, Phys. Rev. **C66**, 015501 (2002).
54. S. Bonetti *et al.*, Nuovo Cimento **A38**, 260 (1977); N. Armenise *et al.*, Nucl. Phys. **B152**, 365 (1979).
55. S.V. Belikov *et al.*, Z. Phys. **A320**, 625 (1985).
56. J. Brunner *et al.*, Z. Phys. **C45**, 551 (1990).
57. J. Carlson *et al.*, Phys. Rev. **C65**, 024002 (2002).
58. H. Gallagher *et al.*, Ann. Rev. Nucl. and Part. Sci. **61**, 355 (2011).
59. G.T. Garvey *et al.*, Phys. Reports **580**, 1 (2015).
60. M. Betancourt, Ph.D. thesis, University of Minnesota,2013.
61. J. Wolcott *et al.*, `arXiv:1509.05729` [hep-ex].
62. L.A. Ahrens *et al.*, Phys. Rev. **D35**, 785 (1987).
63. V.V. Ammosov *et al.*, Z. Phys. **C36**, 377 (1987); O. Erriques *et al.*, Phys. Lett. **70B**, 383 (1977); T. Eichten *et al.*, Phys. Lett. **40B**, 593 (1972).
64. For a compilation of historical coherent pion production data, please see P. Villain *et al.*, Phys. Lett. **B313**, 267 (1993).
65. D. Cherdack, AIP Conf. Proc. **1405**,115(2011).
66. B. Eberly *et al.*, Phys. Rev. **D92**, 092008 (2015).
67. C.T. Kullenberg *et al.*, Phys. Lett. **B706**, 268 (2012).